

Gazi Üniversitesi **Fen Bilimleri Dergisi**PART C: TASARIM VE TEKNOLOJİ

Gazi University Journal of Science PART C: DESIGN AND

TECHNOLOGY



GU J Sci, Part C, 13(3): 981-990 (2025)

Implementation of Battery-Integrated Transformerless High-Gain Smart Inverter

Oğuz ALKUL^{1*} D Şevki DEMİRBAŞ¹ D

¹Gazi University, Graduate School of Natural and Applied Sciences, Department of Electrical and Electronics Engineering, Ankara, Turkey

Article Info

Research article Received: 09/12/2024 Revision: 10/03/2025 Accepted: 24/04/2025

Keywords

Battery Charger Smart Invevrter Power Control Voltage Regulation Smart Inverter Design Transformerless High Gain Converter DC-DC Converter Renewable Energy

Makale Bilgisi

Araştırma makalesi Başvuru: 09/12/2024 Düzeltme: 10/03/2025 Kabul: 24/04/2025

Anahtar Kelimeler

Batarya Şarj Cihazı Akıllı Evirici Güç Kontrolü Gerilim Kontrolü Akıllı İnvertör Tasarımı Transformatörsüz Yüksek kazançlı Dönüştürücü DA-DA Dönüştürücü, Yenilenebilir Enerji

Graphical/Tabular Abstract (Grafik Özet)

This study presents a smart inverter model that includes a battery-integrated, transformerless, and high-gain DC-DC converter capable of bidirectional operation. /Bu çalışma, batarya entegreli, transformatörsüz ve yüksek kazançlı DA-DA dönüştürücü içeren ve iki yönlü çalışabilen akıllı bir invertör modeli sunmaktadır.

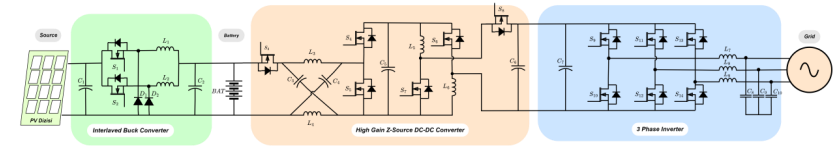


Figure A: Prepared High gain transformerless PV inverter model / Şekil A: Hazırlanan yüksek kazançlı trafosuz PV invertör modeli

Highlights (Önemli noktalar)

- The design, which offers integrated operation between PV panels, battery and grid, supports supply-demand balance with flexible energy storage, transfer and battery charge/discharge control in grid-connected/unconnected modes. / PV paneller, batarya ve şebeke arasında entegre çalışma imkanı sunan tasarım, şebeke bağlantılı/bağlantısız modlarda esnek enerji depolama, aktarım ve batarya şarj/deşarj kontrolü ile arz-talep dengesini destekler.
- The design offers a structure that can operate in grid-connected and unconnected modes, facilitating energy management with battery charge/discharge control. / Tasarum, şebeke bağlantılı ve bağlantısız modlarda çalışabilen, batarya şarj/deşarj kontrolü ile enerji yönetimini kolaylaştıran bir yapı sunmaktadır.
- With advanced control mechanisms, P&O MPPT algorithm and active/reactive power control, maximum power is drawn from PV panels, energy flow is optimized, harmonic distortions and security risks are reduced and safe energy transfer to the grid is ensured./ Gelişmiş kontrol mekanizmaları, P&O MPPT algoritması ve aktif/reaktif güç kontrolü ile PV panellerden maksimum güç çekilir, enerji aktşı optimize edilirken, harmonik bozulmalar ve güvenlik riskleri azaltılarak şebekeye güvenli enerji aktarımı sağlanır.

Aim (Amaç): The study aims to increase energy efficiency and provide safe, flexible energy management in grid-connected/unconnected modes by designing a smart inverter with PV panels and battery integrated, transformerless high-gain DC-DC converter. / Çalışma, PV paneller ve batarya entegreli, transformatörsüz yüksek kazançlı DA-DA dönüştürücülü akıllı inverter tasarlayarak enerji verimliliğini artırıp şebeke bağlantılı/bağlantısız modlarda güvenli, esnek enerji yönetimi sağlamayı amaçlar.

Originality (Özgünlük): Transformerless high-gain smart inverter design offers a unique energy management solution in a compact, efficient and aesthetic structure with PV panels and battery integration. / Transformerless yüksek kazançlı akıllı inverter tasarımı, PV paneller ve batarya entegrasyonuyla kompakt, verimli ve estetik bir yapıda özgün bir enerji yönetimi çözümü sunar.

Results (Bulgular): Effective control at power levels ranging from 1kW to 5kW of the PV inverter, stable DC connection voltage, optimized battery charge/discharge processes and quality grid output verify the performance and reliability of the design. / PV inverterin 1kW'dan 5kW'a kadar değişen güç seviyelerinde etkin kontrol, stabil DC bağlantı gerilimi, optimize edilmiş batarya şarj/deşarj süreçleri ve kaliteli şebeke çıkışı tasarımın performansını ve güvenilirliğini doğrular.

Conclusion (Sonuç): The study reveals that the transformerless high-gain smart inverter provides safe and flexible energy management by increasing energy efficiency with the integration of PV panels and batteries, and offers an effective solution for renewable energy systems. / Çalışma, transformerless yüksek kazançlı akıllı inverterin, PV paneller ve batarya entegrasyonuyla enerji verimliliğini artırarak, güvenli ve esnek enerji yönetimi sağladığını ve yenilenebilir enerji sistemleri için etkili bir çözüm sunduğunu ortaya koymaktadır.



Gazi Üniversitesi **Fen Bilimleri Dergisi**PART C: TASARIM VE TEKNOLOJİ

Gazi University

Journal of Science

PART C: DESIGN AND

TECHNOLOGY



A 8-91 Tables

http://dergipark.gov.tr/gujsc

Implementation of Battery-Integrated Transformerless High-Gain Smart Inverter

Oğuz ALKUL^{1*} Şevki DEMİRBAŞ¹

¹Gazi University, Graduate School of Natural and Applied Sciences, Department of Electrical and Electronics Engineering, Ankara, Turkey

Article Info

Research article Received: 09/12/2024 Revision: 10/03/2025 Accepted: 24/04/2025

Keywords

Battery Charger Smart Invevrter Power Control Voltage Regulation Smart Inverter Design Transformerless High Gain Converter DC-DC Converter Renewable Energy

Abstract

This study presents a novel battery-integrated, transformerless high-gain smart inverter model designed to enhance the efficiency and reliability of photovoltaic (PV) energy systems. The proposed system integrates an interleaved buck converter for battery charging and a transformerless high-gain DC-DC converter operating in parallel with the battery to supply the inverter source. Additionally, a two-level inverter is employed to ensure stable grid voltage generation.

The model incorporates several required control strategies, including Maximum Power Point Tracking (MPPT) for optimal solar energy utilization, active and reactive power control for grid-connected operation, and voltage regulation for off-grid scenarios. The bidirectional energy flow capability enables seamless power distribution between the PV array, battery storage, and the electrical grid, ensuring enhanced system performance. Simulation results validate the efficiency and stability of the proposed inverter model, demonstrating improved power conversion, reduced energy losses, and enhanced system flexibility. By eliminating the need for a transformer, the design achieves higher efficiency and lower cost while maintaining operational reliability. This research contributes to the development of more sustainable and intelligent PV energy solutions, paving the way for improved energy management in renewable power systems.

Batarya Entegreli Transformatörsüz Yüksek Kazançlı Akıllı Evirici Uygulaması

Makale Bilgisi

Araştırma makalesi Başvuru: 09/12/2024 Düzeltme: 10/03/2025 Kabul: 24/04/2025

Anahtar Kelimeler

Batarya Şarj Cihazı Akıllı Evirici Güç Kontrolü Gerilim Kontrolü Akıllı Evirici Tasarımı Transformatörsüz Yüksek kazançlı Dönüştürücü DA-DA Dönüştürücü, Yenilenebilir Enerji

Öz

Bu çalışma, fotovoltaik (PV) enerji sistemlerinin verimliliğini ve güvenilirliğini artırmak için tasarlanmış, bataryaya entegre, trafosuz yüksek kazançlı akıllı evirici modelini sunmaktadır. Önerilen sistem, batarya şarjı için iç içe geçmiş bir azaltan tip dönüştürücü ve evirici kaynağını beslemek için bataryayla paralel çalışan trafosuz yüksek kazançlı DC-DC dönüştürücüyü entegre eder. Ek olarak, kararlı şebeke voltajı üretimini sağlamak için iki seviyeli bir evirici kullanılır.

Model, optimum güneş enerjisi kullanımı için Maksimum Güç Noktası İzleme (MPPT), şebekeye bağlı çalışma için aktif ve reaktif güç kontrolü ve şebekeden bağımsız senaryolar için voltaj düzenlemesi dahil olmak üzere çeşitli gerekli kontrol stratejilerini içerir. Çift yönlü enerji akışı yeteneği, PV dizisi, batarya depolaması ve elektrik şebekesi arasında sorunsuz güç dağıtımını sağlayarak gelişmiş sistem performansı sağlar. Simülasyon sonuçları, önerilen evirici modelinin verimliliğini ve kararlılığını doğrulayarak, iyileştirilmiş güç dönüşümü, azaltılmış enerji kayıpları ve gelişmiş sistem esnekliğini göstermektedir. Bir trafoya olan ihtiyacı ortadan kaldırarak, tasarım operasyonel güvenilirliği korurken daha yüksek verimlilik ve daha düşük maliyet elde eder. Bu araştırma, yenilenebilir enerji sistemlerinde enerji yönetiminin iyileştirilmesinin önünü açarak daha sürdürülebilir ve akıllı PV enerji çözümlerinin geliştirilmesine katkıda bulunmaktadır.

1. INTRODUCTION (GİRİŞ)

Today, growing interest in energy efficiency and sustainable energy sources is driving advancements in energy conversion systems. The significance of inverter technologies is increasingly recognized for ensuring the efficient utilization of renewable

energy sources, particularly solar energy. In this context, battery integrated, transformerless, high-gain smart inverter models are gaining attention due to their advantages in energy storage and conversion processes [1].

Smart inverters, battery chargers, and power control technologies play a crucial role in energy management [2]. These systems offer advanced features for voltage regulation and power optimization [3-4]. Smart inverter designs integrate transformerless high-gain converters alongside high-efficiency reliable converters [5]. They operate in conjunction with DC-DC converters to optimize energy flow. These technologies enhance the efficiency, flexibility, and sustainability of energy systems [4-5].

Transformerless inverters are widely used in the energy sector due to their high efficiency and low cost. These inverters enable more compact and lightweight designs, reducing both space and cost compared to transformer-based inverters [6-7]. However, transformerless inverters face challenges such as harmonic distortions and safety risks during grid connection [8]. To mitigate these issues and enhance system efficiency, the smart control systems play a crucial role.

Battery integration helps balance energy supply and demand by providing flexibility in energy storage and utilization. Energy storage systems are particularly critical for integrating intermittent renewable energy sources. Since solar energy reaches peak efficiency during daylight hours but ceases production at night, battery systems become essential. The large-scale integration of intermittent renewables significantly impacts traditional generation technologies and the electrical grid. Such

energy sources require flexible generation capacities capable of rapid response to maintain supply-demand balance [9].

Previous studies in the literature have extensively examined transformerless inverter technologies, energy storage integration, and smart control mechanisms to enhance system efficiency and reliability [1-9]. Research has highlighted the role of high-gain DC-DC converters in improving energy conversion, while interleaved buck converters have been widely explored for their benefits in reducing power loss and increasing efficiency in PV systems. Additionally, LC filters have been commonly utilized to mitigate harmonic distortions and optimize inverter performance [10-12].

Building upon these studies, this article examines a battery-integrated transformerless high-gain smart inverter model, its operating principles, and its advantages. Specifically, the study focuses on a traditional six-switch inverter model. transformerless high-gain DC-DC converter, and a two-cell interleaved converter. The inverter design was selected considering power, efficiency, and cost performance. Furthermore, an LC filter was implemented at the output to minimize harmonic distortions and improve system performance. The research also evaluates the application of interleaved buck converters in PV systems, emphasizing their role in enhancing efficiency and reliability.

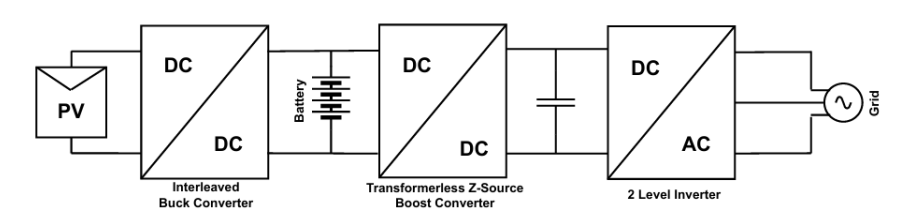


Figure 1. General block diagram of PV inverter (PV invertörünün genel blok seması)

In this study as illustrated in the general block diagram in Figure 1, a group of PV panels is connected to a battery via an MPPT-controlled buck converter. The high voltage required for the inverter, which significantly exceeds the battery voltage and supports bidirectional operation, is achieved through a boost converter. This high voltage is then integrated into the grid via a two-level inverter.

The introduction section presents the preferred converter block diagram, providing readers with a general structural framework of the work. The second section discusses the transformerless PV

inverter topology, and the modeling approach based on this topology. The third section examines the components of the smart inverter and their respective functions in detail. The fourth section focuses on control mechanisms and their operating principles. Finally, the fifth section presents the simulation results, evaluating the outcomes and findings of the study.

2. TRANSFORMERLESS SMART PV INVERTER DESIGN (TRANSFORMATÖRÜSÜZ AKILLI PV EVİRİCİ TASARIMI)

Within the scope of this research, six seriesconnected PV panels were used to supply a battery through a single interleaved buck converter employing a maximum power point tracking (MPPT) algorithm. The system, modeled in Figure 2, is designed to maximize the efficient utilization of energy generated by the solar panels. A bidirectional, transformerless Z-Source converter, connected in parallel with the battery, supplies the DC link. This converter optimizes energy flow within the system by enabling bidirectional energy transfer both from the battery to the PV panels and from the rectified grid voltage back to the battery. The transformerless design provides significant advantages, including reduced energy losses,

simplified control mechanisms, and lower production costs. The DC link is then integrated into the grid through a two-level full-bridge inverter designed for power regulation. This inverter is controlled to manage power flow within the DC link while ensuring that the voltage and frequency are appropriately synchronized with the grid. As a result, energy balance within the system is maintained, and electricity is reliably transmitted to the grid. This integrated structure enhances the efficiency of energy storage, conversion, and integration, ultimately enabling a more effective and sustainable use of solar energy.

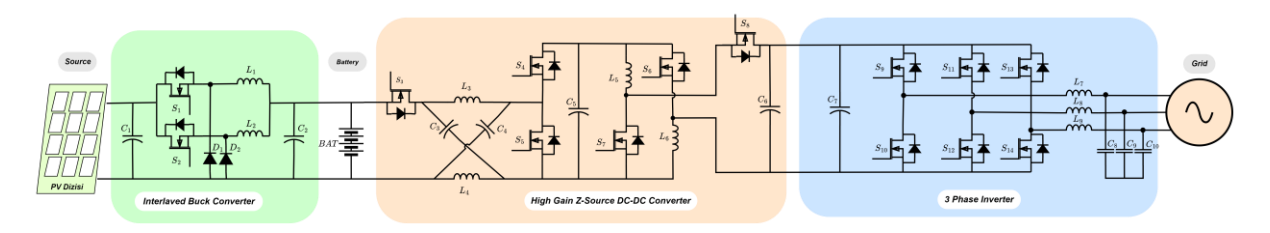


Figure 2. Prepared high gain transformerless PV inverter model (Hazırlanan yüksek kazançlı transformatörsüz PV evirici modeli)

In the MPPT section of the developed smart PV converter, advanced monitoring applications, including P&O (Perturb and Observe) method were implemented. approach This ensures efficiency by continuously tracking and adjusting to the maximum power fluctuations of the PV panel. Additionally, a PI (Proportional-Integral) controller was employed to regulate the charging process and optimize the converter's current and voltage expansion, ensuring the most suitable operating conditions. This control mechanism not only stabilizes the battery voltage but also maintains a consistent voltage level on the DC link connected to the converter.

In the inverter section, direct power control is applied during grid-connected operation. The converter monitors its voltage and frequency to ensure proper power delivery to the grid. Moreover, Moreover, the inverter voltage control parameters dynamically adjust in response to system conditions, guaranteeing a stable energy supply. This design allows the converter to maintain continuous and uninterrupted power delivery in both grid-connected and stand-alone modes. Additionally, when the PV panel voltage and battery charge levels are sufficient, the system operates with Uninterruptible Power Supply (UPS) functionality, ensuring a constant power supply and reliable energy consumption management.

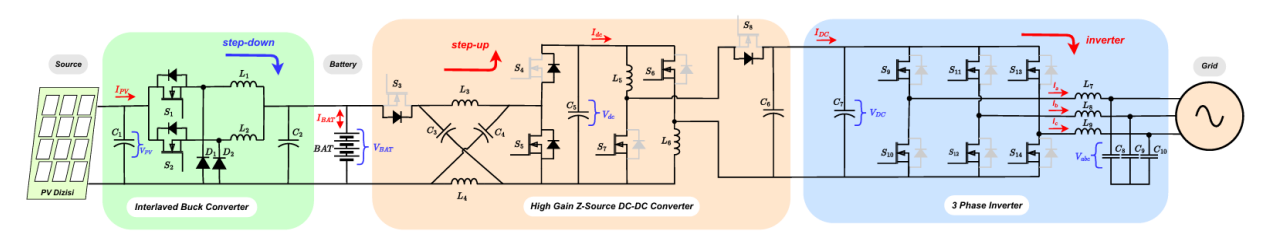


Figure 3. Feeding the grid with battery-backed PV panels (Sebekenin batarya destekli PV panelleriyle beslenmesi)

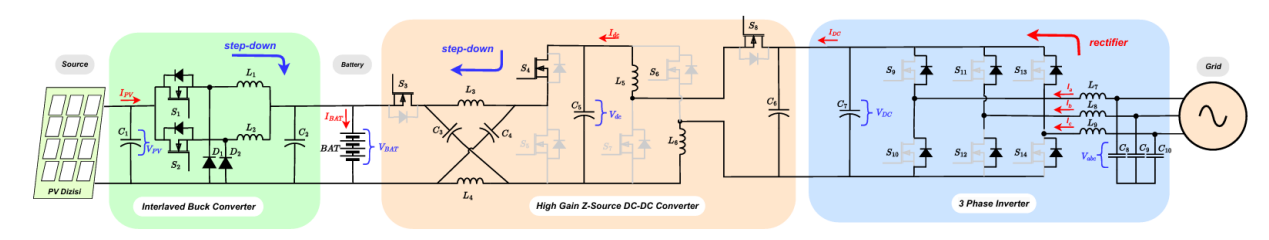


Figure 4. Battery charging with PV panels and grid (PV panelleri ve şebeke ile batarya şarjı)

When PV panels and batteries supply energy to the grid, the PV converter tracks the maximum power point and transfers the highest possible energy to the battery (Figure 3). During this process, the battery can be charged by controlling the PV panels. However, when PV energy is insufficient or unavailable, the grid voltage is directly rectified into DC voltage and transferred to the battery through a step-down converter operating as a transformerless Z-source converter. The working principle of this method is illustrated in Figure 4.

A carefully selected configuration was implemented for PV panel connections, prioritizing system efficiency and safety. In this context, a 2-series and 3-parallel connection scheme was chosen for the model. This configuration was selected to effectively increase voltage while ensuring balanced current distribution. The solar panel connection layout is illustrated in Figure 5.

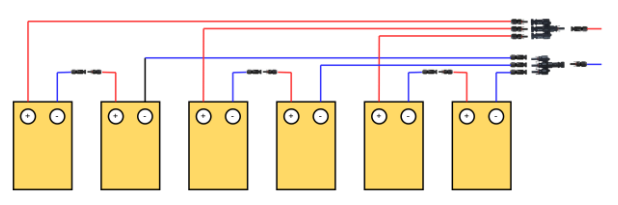


Figure 5. Connection diagram of solar panels (Güneş panellerinin bağlantı şeması)

3. DESIGN (TASARIM)

2.1. Interleaved Buck Converter (İki Hücreli Azaltan Tip Dönüştürücü)

Interleaved buck converter input and output filter parameters are determined according to the desired power values. The parameters used in the study are given in Table I.

Table 1. Interleaved Buck Converter Parameters (İki hücreli azaltan tip dönüştürücü Parametreleri)

Circuit Elements	Values
Input Voltage (V_{IN})	90 V
Output Voltage (V_{OUT})	55 V
Input Surge Voltage (ΔV_{IN})	1Vpp
Output Surge Voltage (ΔV_{OUT})	100mVpp
Converter Power (W_{MAX})	3 kVA
Switching Frequency (f_{SW})	5 kHz
Switching Rating (V_{GES}) (200 V
Switching Rating (I_C)	25A @ 100° C
Input Capacitor (C_{IN})	6 * 470 μF
Output Capacitor (C_{OUT})	$1 * 470 \mu F$
Inductor Value (L)	4 mH

 a) Inductor Selection: In determining the value of the buck-type converter parameters, the inductor L was calculated using the Equation 1 [13].

$$L = \frac{V_{OUT} \times (1 - D)}{f_{SW} \times I_{PP}} = \frac{55 \times (1 - 55V/90V)}{5kHz \times 1A} = 4.27mH \quad (1)$$

Here, V_{OUT} is the output voltage, D is the switching duty ratio, f_{SW} is the switching frequency, and I_{PP} is the ripple amount of the output current.

b) Capacitor Selection: The input capacitor value was calculated using Equation 2 and the output capacitor values were calculated using Equation 4 [13].

$$C_{INphase} = \frac{I_{PHASEmax} \times D \times n(1-D)}{f_{SW} \times \Delta V_{IN}}$$
 (2)

$$C_{INphase} = \frac{3kW/(2\times55V)\times0.61\times2(1-0.61)}{5kHz\times1V_{PP}} = 2595\mu F$$
 (3)

Here, $C_{INphase}$ is the capacitor value calculated for each phase, $C_{PHASEmax}$ is the maximum phase current, D is the maximum switching duty ratio, n is the phase number, f_{SW} is the switching frequency, and ΔV_{IN} is the ripple voltage amount of the input voltage value.

$$C_{OUT} = \frac{I_{PP}}{8 \times f_{SW} \times \Delta V_{OUT}} \tag{4}$$

$$C_{OUT} = \frac{I_{PP}}{8 \times 5kHz \times 100mV_{PP}} = 250\mu F \tag{5}$$

2.2. Z-source Transformerless High Gain

Converter(Z-kaynaklı Trafosuz Yüksek Kazançlı Dönüştürücü)

The converter model presented in [14], which has an efficiency of over 96 percent, which is a high rate among DC-DC converters, was preferred.

The input voltage in the converter used is V_{IN} , output voltage is V_{OUT} and switching duty ratio is D, input and output factor are given in Equation 6 [14].

$$V_{OUT} = \frac{1+D}{(1-D)^2} V_{IN} \tag{6}$$

The input and output factors of the Z-source converter according to the switching duty ratio are given in Equation 7 [15].

$$V_{OUT} = \frac{1}{(1-2D)} V_{IN} \tag{7}$$

The output ratio obtained as a result of switching from the formulas in Equation 6 and Equation 7 is given in Equation 8.

$$V_{OUT} = \frac{(1+D)}{(1-D)^2(1-2D)} V_{IN}$$
 (8)

 a) Inductor Selection: The Z source is directly connected to the boost converter and used at the inverter input. The coil calculation of the Z source is given in Equation 9.

$$L_{ZSource} = \frac{2 \times D \times V_{OUT} \times (1 - D)}{3 \times \Delta I_{OUT} \times m \times I_L \times cos\theta \times f_{SW}}$$
(9)

$$L_{ZSource} = \frac{2 \times 0.5 \times 450 V \times (1 - 0.5)}{3 \times 2.5 A \times 0.5 \times 11.1 A \times 1 \times 1 kHz} = 2.7 mH \ (10)$$

Here, assuming that the inverter operates under normal conditions, the duty ratio (D) and the inverter modulation index (m) are both set to 0.5. Additionally, the output inverter current, which depends on the power drawn from the specified source, as denoted I_L , while the inverter power factor is represented as $cos\theta$. The inductor current ripple value is expressed as a percentage and denoted as ΔI_{OUT} , whereas the the switching frequency used in the Z-source converter is represented as f_{SW} .

b) Capacitor Selection: The capacity calculation of the Z-source is given in Equation 11.

$$C_{ZSource} = \frac{3 \times D \times m \times I_L \times cos\theta}{8 \times \Delta V_C \times V_{OUT} \times (1-D) \times f_{SW}}$$
(11)

$$C_{ZSource} = \frac{{}_{3\times0.5\times0.5\times11.1A\times1}}{{}_{8\times0.5V\times450V\times(1-0.5)\times1kHz}} = 4630\mu F$$
 (12)

Here, $\Delta \hat{V}_C$, which is not expressed in the formula, represents the capacitor voltage ripple value as a percentage

2.3. Traditional 2-Stage Inverter (Geleneksel 2 Seviyeli Evirici)

The peak voltage \hat{v}_{ac} in a 2-level inverter, where *D* represents the switching duty ratio, can be calculated with the formula below [16].

$$\hat{v}_{ac} = m \frac{V_{DC}}{2} \tag{13}$$

Here, \hat{v}_{ac} represents the peak phase voltage value and m represents the modulation index value of the inverter. Using this equation, the gain ratio can be expressed with the following equation [16].

$$G = \frac{\hat{v}_{ac}}{V_{DC}/2} = \frac{m}{1 - D} \tag{14}$$

a) Inductor Selection: The equality in Equation 15 was used in the selection of the coil used in the inverter [12].

$$L = \frac{1}{8} \frac{V_{DC}}{\Delta \hat{I}_L \times f_{SW}} = \frac{1}{8} \frac{450V}{1.1A \times 5kHz} = 10mH$$
 (15)

Here, L represents the inductor value, V_{DC} represents the inverter input voltage, $\Delta \hat{I}_L$ represents the current ripple value, and f_{SW} represents the inverter switching frequency value.

b) Capacitor Selection: The selected capacitance value should be higher than the resonance frequency of the LC filter. Accordingly, the resonance capacitance value can be determined using Equation 16 [12]. Based on the appropriate circuit configuration, the capacitance value was selected using the equation given in Equation 17 [17].

$$C > \left(\frac{1}{f_{SW}2\pi}\right)^2 \frac{1}{L} = \left(\frac{1}{5kHz \times 2\pi}\right)^2 \frac{1}{10mH} = 0.1\mu F$$
 (16)

$$C = \frac{2 \times P}{f_{SW} \times V_{DC} \times \Delta V_{ac}} = \frac{2 \times 5kW}{5kHz \times 450V \times 30V} = 14\mu F \quad (17)$$

Accordingly, the filter capacitance value was selected as 22uF for availability and widespread use. Here, f_{SW} represents the switching frequency, L represents the inductance value calculated from Equation 15, and ΔV_{ac} represents the maximum deviation voltage allowed at the output voltage. The ΔV_{ac} value expressed here was selected according to the power quality standards given by IEEE-1547, IEEE-519 standards.

The parameters used in the simulation are given in Table 2.

Table 1. Simulation parameters (Benzetim parametreleri)

System Parameters	Values
Simulation Step Time (T_S)	50x10-6 s
PV Panel Power (P_{pv})	6x545W
Grid Voltage (V_{grid})	115VAC
Utility Grid Frequency (f)	50Hz
DC Line Voltage (V_{out})	450VDC
Nominal Power (P)	5kW
Battery Voltage (V_{bat})	48V
Battery Capacity (Ah)	100Ah
Inverter Inductor Value	10mH
(L_1,L_2,L_3)	
Inverter Filter Capacitor	22μF
(C_7, C_8, C_9)	
Switching Frequency (f_{SW})	5kHz
Capacitances of C_1 , C_2 , C_3 C_6	$470\mu F$

3. CONTROL (KONTROL)

In the study, the voltage generated by the PV panels was optimized using the Maximum Power Point Tracking (MPPT) technique and integrated into the battery through an interleaved buck converter. The battery supplied via a transformerless Z-Source DC-DC converter and a controlled inverter connected to the grid.

3.1. MPPT Control (MPPT Kontrolü)

P&O (Perturb and Observe) is an MPPT method that enables solar panels to operate at maximum efficiency. The P&O method utilizes a simple yet effective algorithm. This algorithm incrementally increases or decreases the output voltage of the solar panel at regular intervals and monitors the resulting change in power output. If the power output increases, the adjustments continue in the same direction; however, if the power output decreases, the direction of adjustment is reserved. This process continues until the maximum power point is reached. The control algorithm used in the control section is illustrated in Figure 6.

```
function Vref = RefGen(V, I, Vrefmax, Vrefmin,
deltaVref = 1:
persistent Vold Pold Vrefold;
dataType = 'double';
if isempty(Vold)
    Vold = 0;
    Pold = 0;
     Vrefold = Vrefinit:
dV = V - Vold;
dP = P - Pold;
      if dP<0
          if dV<0
               Vref = Vrefold + deltaVref;
               Vref = Vrefold - deltaVref;
          end
               Vref = Vrefold - deltaVref;
               Vref = Vrefold + deltaVref;
         end
else Vref = Vrefold;
end
if Vref >= Vrefmax | Vref <= Vrefmin
    Vref = Vrefold;</pre>
Vrefold = Vref;
Vold = V;
Pold = P;
```

Figure 6. P&O MPPT algorithm (P&O MPPT algoritması)

3.2. Active Reactive Power Control (Aktif Reaktif Güç Kontrolü)

In the inverter developed for PV systems, a controller model capable of active and reactive power control was implemented to optimize grid

efficient compatibility and ensure management. With the help of this controller, the energy obtained from the battery and PV panels is supplied directly to the grid in a controlled manner based on demand. Additionally, setting the reference values in this controller unit to negative enables the inverter to function as a rectifier. This feature allows the battery to be act as an energy storage unit rather than a power source. The Matlab/Simulink model, which demonstrates the inverter's ability to control active and reactive power based on reference values is shown in Figure 7 [18].

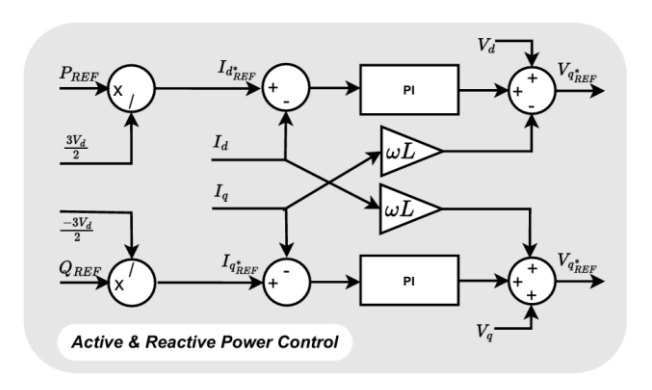


Figure 7. Active reactive power control model [18] (Aktif reaktif güç kontrol modeli [18])

3.3. Voltage Control (Gerilim Kontrolü)

When the grid is disconnected, the smart converter switches to voltage control to enable off-grid operation. This allows the system to regulate voltage independently of the grid. The Matlab/Simulink control model used for this process is shown in Figure 8. [19].

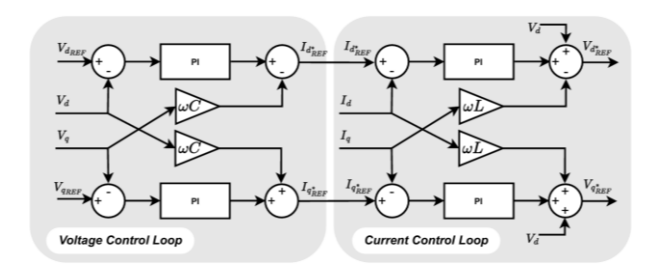


Figure 8. Voltage current control model [19] (Gerilim akım kontrol modeli [19])

3.4. Battery Charge & Discharge Control (Batarya Şarj & Deşarj Kontrolü)

Numerous studies have been conducted on charge and discharge control for 100Ah 48V battery. These studies primarily focus on aspects such as the electrical properties of batteries, charge/discharge algorithms, energy management strategies and

safety measures. The findings contribute to the more efficient and safer utilization of battery technologies [20-21].

In battery charging and discharging applications, direct PI control is employed. Since the system operates as a grid-interactive solution, it remains under continuous control. Charge and discharge current limits are maintained according to predefined battery specifications. The control structure is illustrated in Figure 9.

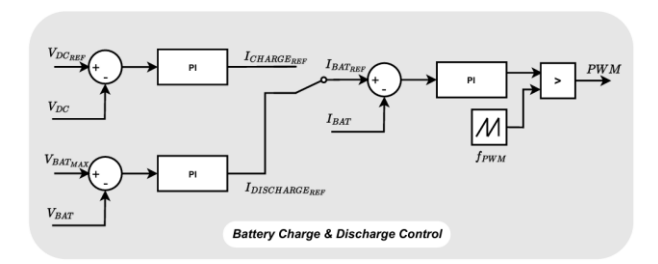


Figure 9. Battery charge and discharge control (Akü şarj ve deşarj kontrolü)

The control structure consists of 3 parts. In the first working method, when there is sufficient power in PV, $(P_{PV} > P_{BAT_{CHARGE}})$ the device controls the power and charges the battery as much as the grid production amount and sends the remaining energy to the grid. In the second working method, when the power produced in PV is insufficient to feed the grid, $(P_{PV} < P_{GRID_{NEED}})$ the required energy is met by the batteries $(P_{GRID_{NEED}} = P_{PV} + P_{BAT})$. In the last working method, the energy produced from PV systems and the excess energy needed by the grid are stored in the batteries $(P_{BAT_{CHARGE}} = P_{PV} + P_{GRID})$. The operating states of the system are given in Figure 3 and Figure 4.

$$P_{PV} \ge P_{BAT_{CHARGE}} + P_{GRID_{NEED}} \tag{18}$$

$$P_{GRID} \ge P_{BAT_{CHARGE}} + P_{GRID_{NEED}} \tag{19}$$

$$P_{BAT_{CHARGE}} = > P_{PV} + P_{GRID}$$
 (20)

4. EXPERIMENTS (DENEYLER)

The research results include simulation data obtained during the operation of solar inverters. Figure 11 presents detailed MPPT control results of the PV inverter, while Figure 10 illustrates the energy transfer from the inverter to the grid. Figure 12 depicts the voltage, current and charge status of

the battery during charging and discharging processes, whereas Figure 13 analyzes the DC link voltage control and current. The voltage and current variations at the inverter output are shown in Figure 14a. Finally, Figure 14b displays the dynamic response of the inverter, including output voltage and current. These results are used to evaluate the design and performance of the solar inverter system and demonstrate its operational capability.

In the simulation study, the inverter was operated with the control method given in Figure 7. The control response of the inverter was examined at 1kW, 4kW, 2kW, 5kW and finally 1kW again, at 2-second intervals. The simulation result obtained is given in Figure 10. Here, P_{REF} is the reference power value and P is the output power of the inverter.

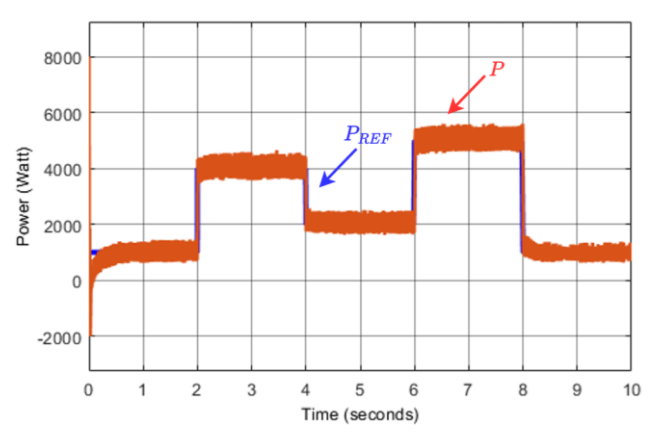


Figure 10. Power time graph of energy transmitted to the grid (Sebekeye iletilen enerjinin güç-zaman grafiği)

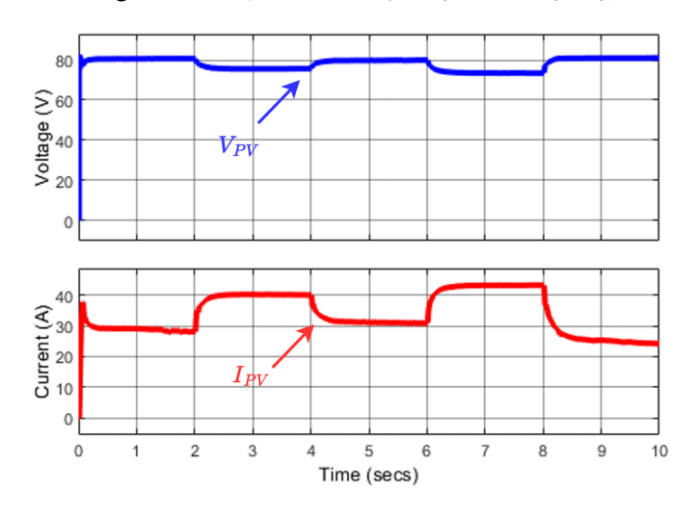


Figure 11. Voltage and current graph of solar panels as a result of MPPT applied (MPPT uygulaması sonucu güneş panellerinin gerilim ve akım grafiği)

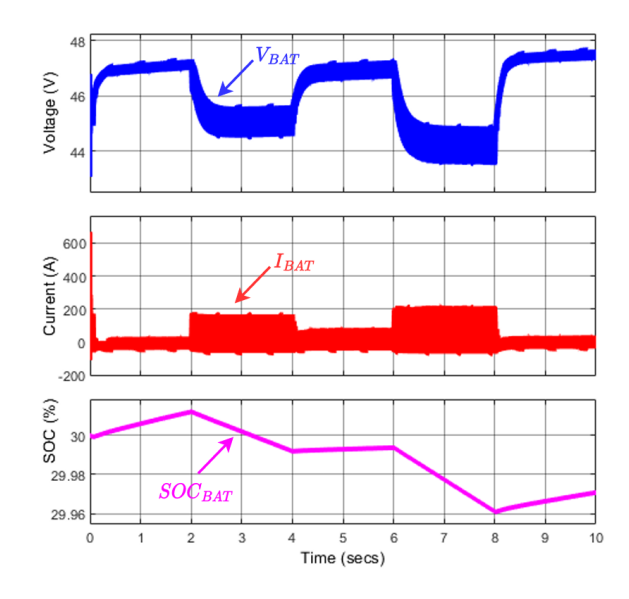


Figure 12. Battery voltage, current and SOC (Batarya voltaji, akımı ve SOC)

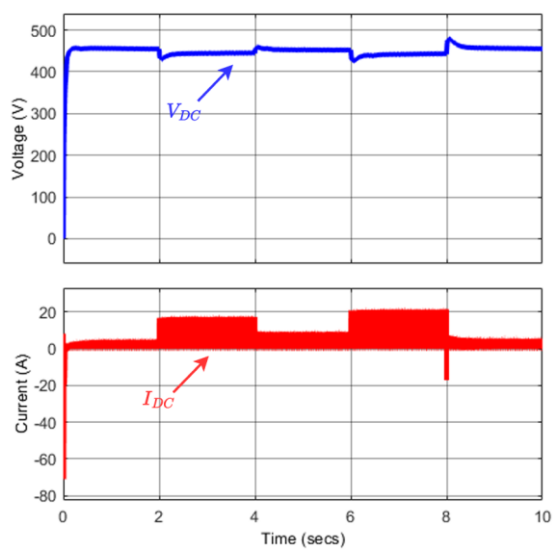


Figure 13. DC link voltage and current result (DC bağlantı voltajı ve akım sonucu)

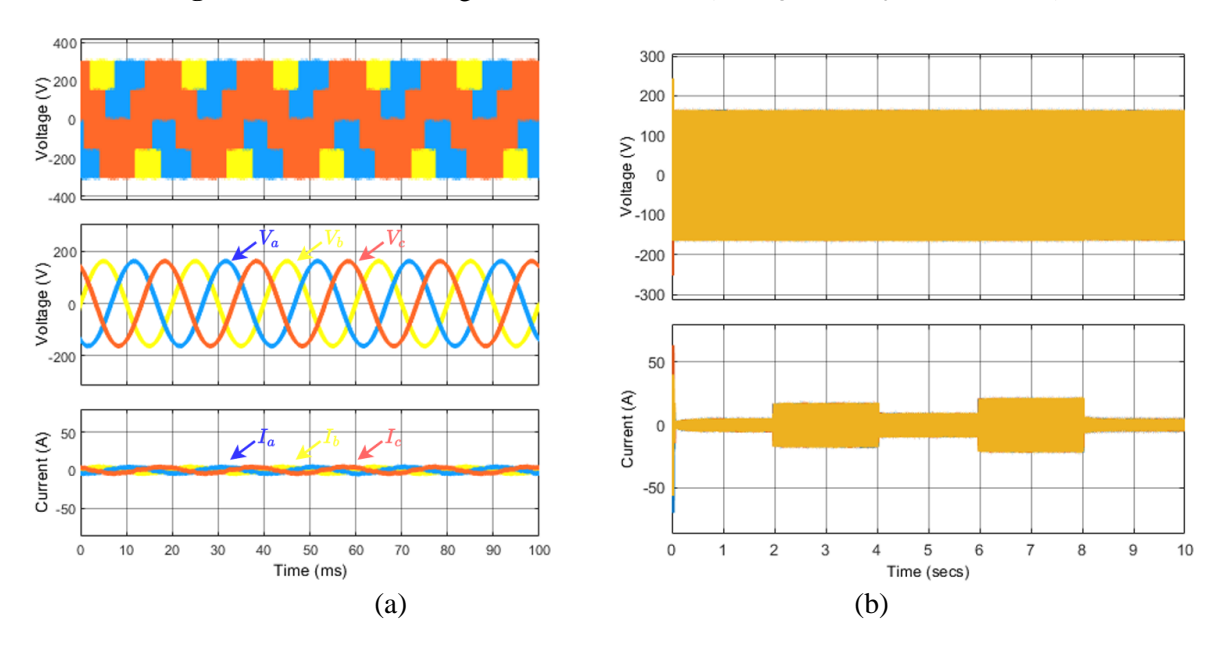


Figure 14. (a) Inverter voltage and current output, (b) Inverter dynamic response output voltage and current ((a) Evirici voltajı ve akım çıkışı, (b) Evirici dinamik tepki çıkış voltajı ve akımı)

The proposed battery-integrated, transformerless high-gain smart inverter model demonstrates significant improvements in efficiency, reliability, and energy management for PV systems. Through advanced control strategies such as MPPT, voltage regulation, and bidirectional power flow, the system ensures optimal utilization of solar energy while supporting grid stability. The incorporation of a high-gain DC-DC converter and an interleaved buck converter further enhances power conversion efficiency, reducing losses and improving energy storage capabilities.

Simulation results validate the effectiveness of the proposed design, showcasing its potential for real-world applications in both grid-connected and off-grid scenarios. While this study highlights the advantages of transformerless inverter technology, further research is needed to address potential challenges such as safety considerations and grid compatibility enhancements. Future work will focus on refining the control algorithms and optimizing the hardware implementation to facilitate wider adoption of this technology in renewable energy systems.

5. **CONCLUTIONS** (SONUÇLAR)

The proposed battery-integrated, transformerless high-gain smart inverter model demonstrates significant improvements in efficiency, reliability, and energy management for PV systems. Through advanced control strategies such as MPPT, voltage regulation, and bidirectional power flow, the system ensures optimal utilization of solar energy while supporting grid stability. The incorporation of a high-gain DC-DC converter and an interleaved buck converter further enhances power conversion efficiency, reducing losses and improving energy storage capabilities.

Simulation results validate the effectiveness of the proposed design, showcasing its potential for real-world applications in both grid-connected and off-grid scenarios. While this study highlights the advantages of transformerless inverter technology, further research is needed to address potential challenges such as safety considerations and grid compatibility enhancements. Future work will focus on refining the control algorithms and optimizing the hardware implementation to facilitate wider adoption of this technology in renewable energy systems.

ACKNOWLEDGMENTS (TEŞEKKÜR)

The research article was supported by Gazi University under project code FBA-2023-8164. The authors extend their gratitude for this support.

DECLARATION OF ETHICAL STANDARDS (ETİK STANDARTLARIN BEYANI)

The author of this article declares that the materials and methods they use in their work do not require ethical committee approval and/or legal-specific permission.

Bu makalenin yazarı çalışmalarında kullandıkları materyal ve yöntemlerin etik kurul izni ve/veya yasal-özel bir izin gerektirmediğini beyan ederler.

AUTHORS' CONTRIBUTIONS (YAZARLARIN KATKILARI)

Oğuz ALKUL: He conducted the experiments, analyzed the results and performed the writing process.

Deneyleri yapmış, sonuçlarını analiz etmiş ve makalenin yazım işlemini gerçekleştirmiştir.

Şevki DEMİRBAŞ: He evaluated the results and participated in the preparation and improvement of the draft of the article.

Sonuçları değerlendirdi ve makale taslağının hazırlanmasında ve geliştirilmesinde görev aldı.

CONFLICT OF INTEREST (ÇIKAR ÇATIŞMASI)

There is no conflict of interest in this study.

Bu çalışmada herhangi bir çıkar çatışması yoktur.

REFERENCES (KAYNAKLAR)

- [1] D. Parra, M. K. Patel, Effect of tariffs on the performance and economic benefits of PV-coupled battery systems. Applied Energy, 164 (2016) 175-187.
- [2] A. M. Mahfuz-Ur-Rahman, et al., An effective energy management with advanced converter and control for a PV-battery storage based microgrid to improve energy resiliency. IEEE Transactions on Industry Applications, 57:6 (2021) 6659-6668.
- [3] S. Y. Mousazadeh Mousavi, et al., Power quality enhancement and power management of a multifunctional interfacing inverter for PV and battery energy storage system. International Transactions on Electrical Energy Systems, 28:12 (2018) e2643.

- [4] D. Barater, et al., Recent advances in singlephase transformerless photovoltaic inverters. IET Renewable Power Generation, 10:2 (2016) 260-273.
- [5] S. Saridakis, E. Koutroulis, F. Blaabjerg, Optimal design of modern transformerless PV inverter topologies. IEEE Transactions on Energy Conversion, 28:2 (2013) 394-404.
- [6] M. F. Kibria, et al., A comparative review on single-phase transformerless inverter topologies for grid-connected photovoltaic systems. Energies, 16:3 (2023) 1363.
- [7] O. Alkul, Ş. Demirbaş, Review of the solid-state transformers and an application of full bridge DC/DC converter. Gazi Üniversitesi Fen Bilimleri Dergisi Part C: Tasarım ve Teknoloji, 7:2 (2019) 450-471.
- [8] M. Shayestegan, et al., An overview on prospects of new generation single-phase transformerless inverters for grid-connected photovoltaic (PV) systems. Renewable and Sustainable Energy Reviews, 82 (2018) 515-530.
- [9] MIT Energy Initiative, Managing Large-Scale Penetration of Intermittent Renewables, (2012).
- [10] S. Adak, Harmonics mitigation of standalone photovoltaic system using LC passive filter. Journal of Electrical Engineering & Technology, 16:5 (2021) 2389–2396.
- [11] S. Dlamini, I. E. Davidson, A. A. Adebiyi, Design and application of the passive filters for improved power quality in stand-alone PV systems. 2023 31st Southern African Universities Power Engineering Conference (SAUPEC), IEEE, (2023) 1–6.
- [12] K. H. Ahmed, S. J. Finney, B. W. Williams, Passive filter design for three-phase inverter interfacing in distributed generation. 2007 Compatibility in Power Electronics, IEEE, (2007).
- [13] C. Parisi, Multiphase buck design from start to finish (Part 1). Texas Instruments, Application Report SLVA882, 55 (2017).
- [14] H. Y. Ahmed, O. Abdel-Rahim, Z. M. Ali, New high-gain transformerless DC-DC boost converter system. Electronics, 11:5 (2022) 734.
- [15] M. Zhu, K. Yu, F. L. Luo, Switched inductor Z-source inverter. IEEE Transactions on Power Electronics, 25:8 (2010) 2150-2158.
- [16] A. Ayad, S. Hanafiah, R. Kennel, A comparison of quasi-Z-source inverter and traditional two-stage inverter for photovoltaic application. Proceedings of PCIM Europe 2015; International Exhibition and Conference for Power Electronics, Intelligent Motion, Renewable Energy and Energy Management, VDE, (2015).

- [17] Y. V. Pavan Kumar, R. Bhimasingu, Design of voltage and current controller parameters using small signal model-based pole-zero cancellation method for improved transient response in microgrids. SN Applied Sciences, 3 (2021) 1-17.
- [18] M. M. B. Tappeh, J. S. Moghani, A. Khorsandi, Active and reactive power control strategy of the modular multilevel converter for grid-connected large-scale photovoltaic conversion plants. 2019 10th International Power Electronics, Drive Systems and Technologies Conference (PEDSTC), IEEE, (2019).
- [19] E. Choque Pillco, L. F. C. Alberto, R. V. de Oliveira, Time scale stability analysis of a Hopf bifurcation in a wind–diesel hybrid microgrid. IET Renewable Power Generation, 14:9 (2020) 1491-1501.
- [20] P. K. Atri, P. S. Modi, N. S. Gujar, Design and development of solar charge controller by implementing two different MPPT algorithm. 2021 International Conference on Advances in Electrical, Computing, Communication and Sustainable Technologies (ICAECT), IEEE, (2021).
- [21] A. Maliat, M. A. Mahmud, M. A. Razzak, Design and analysis of a 48V on-board fast charging system for electric vehicles. 2021 Innovations in Power and Advanced Computing Technologies (i-PACT), IEEE, (2021).